

Diversity waves in collapse-driven population dynamics

Sergei Maslov*

*Biological, Environmental and Climate Sciences Department,
Brookhaven National Laboratory,
Upton, NY 11973, USA*

Kim Sneppen†

*Center for Models of Life, Niels Bohr Institute,
University of Copenhagen,
2100 Copenhagen, Denmark*

(Dated: April 27, 2019)

Populations of species in ecosystems are constrained by the availability of resources within their environment. In effect this means that a growth of one population, needs to be balanced by the reduction in size of others. In neutral models of biodiversity all populations are assumed to change incrementally due to stochastic births and deaths of individuals. Here we propose and model another redistribution mechanism driven by abrupt collapses of the entire population of a single species freeing up resources for the remaining ones. This mechanism may be relevant for communities of bacteria, with strain-specific collapses caused e.g. by invading bacteriophages, or for other ecosystems where infectious diseases play an important role.

The emergent property of the population dynamics in our system are cyclic “diversity waves” triggered by collapses of globally dominating populations. The population diversity in the environment peaks at the beginning of each wave and exponentially decreases afterwards. Population sizes in our system follow a bimodal distribution with the lower peak composed of the recently collapsed or the newly arrived species. In contrast to this, the upper peak of the distribution consists of the surviving species in the current diversity wave. The populations of the most abundant species in the upper peak exhibit a scale-free distribution with a nearly universal exponent of about 1.7. We show that our model is robust with respect to variations in dynamical rules including gradual redistribution of populations between subsequent collapses and variation in species’ growth or collapse rates.

Author Summary

The rate of unlimited exponential growth is traditionally used to quantify fitness of species or success of organizations in biological and economic context respectively. However, even modest population growth quickly saturates any environment. Subsequent resource redistribution between the surviving populations is assumed to be driven by incremental changes due to stochastic births and deaths of individuals. Here we propose and model another redistribution mechanism driven by collapses of the entire populations freeing up resources for the growth of others. The emergent property of our dynamics are cyclic “diversity waves” triggered by a collapse of the globally dominating population. Gradual extinctions of species within the current wave results in the scale-free population size distribution of the most abundant species. Our study offers insights to population dynamics of microbial communities with local collapses caused e.g. by invading bacteriophages. It also provides a simplified dynamical description of companies competing in an economic sector with frequent rate of bankruptcy.

Introduction

Mathematical description of many processes in biology and economics or finance assumes long-term exponential growth [1, 2] yet no real-life environment allows growth to continue forever [3, 4]. In biology any growing population eventually ends up saturating the carrying capacity of its environment determined e.g. by nutrient availability. The same is true in economics where availability of new customers and/or natural resources inevitably sets a limit on growth of companies. Population dynamics in saturated environments is routinely described by neutral “community drift” models [5, 6] sometimes with addition of deterministic differences in efficiency of utilizing resources [7].

Here we introduce and model the saturated-state dynamics of populations exposed to episodic random collapses. All species are assumed to share the same environment that ultimately sets the limit to their exponential growth. Examples of such systems include local populations of either a single or multiple biological species competing for the same nutrient, companies competing to increase their market shares among a limited set of customers, etc. Specific case studies can be drawn from microbial ecology where susceptible bacteria are routinely decimated by exposure to bacteriophages (see e.g. [8, 9] and references therein), or paleontological record, where entire taxonomic orders can be wiped out by sudden extinctions happening at a rate independent of order size

* ssmaslov@gmail.com

† ksneppen@gmail.com

[10].

Results

Population growth $P(t)$ of a single exponentially replicating species in a growth-limiting environment is traditionally described by Verhulst's or logistic equation $dP/dt = \Omega \cdot P \cdot (1 - P/P_{tot})$ [4], where the carrying capacity of the environment P_{tot} without loss of generality can be set to 1. In this paper we consider the collective dynamics of multiple populations competing for the same rate-limiting resource:

- Local populations are subject to episodic random collapses or extinctions. The probability of an extinction is assumed to be independent of the population size. Immediately after each collapse the freed-up resources lead to the transient exponential population growth of all remaining populations P_j . The growth stops once the global population $\sum_j P_j$ reaches the carrying capacity $P_{tot} = 1$.
- The environment is periodically reseeded with new species starting from the same small population size $\gamma \ll 1$ (measured in units of environment's carrying capacity).
- We initially assume that the growth rates and collapse probabilities of all local populations are equal to each other. We also disregard the neutral drift [5] in sizes of individual populations during the time between subsequent collapses. All these assumptions will be discussed later in the paper and simulated in the Supplementary Materials.

The number of species in the steady state of the model is determined by the competition between the constant rate of introduction of new species and the overall rate of extinctions in the environment that is proportional to the number of species. To simplify our modeling we will consider a closely related variant of the model in which the number of species N is kept strictly constant. In this case each extinction event is immediately followed by the introduction of a brand new species. We have verified that the two version of our model have very similar steady state properties.

The dynamics of the fixed- N model is described by

$$dP_i/dt = \Omega \cdot P_i \cdot (1 - \sum_j P_j) - \eta_i(t) \cdot P_i \quad , \quad (1)$$

where $\eta_i(t)$ is the random variable which is equal to zero for surviving populations and has a large positive value for populations undergoing a collapse.

To speed up our simulations we do not continuously calculate Eq. (1) since most of the time the carrying capacity of the environment is saturated when local populations do not change. Instead we simulate the model at

discreet time steps marked by extinction events. At every time step a randomly selected local population goes extinct and a brand new species with population $\gamma \ll 1$ is added to the environment. We then instantaneously bring the system to its the carrying capacity by multiplying all populations by the same factor.

In spite of its simplified description of the ecosystem disregarding pairwise interactions between species our model has a rich population dynamics. Fig. 1A shows the time-courses of populations in a system with $N = 20$ species and $\gamma = 10^{-4}$. At certain times the carrying

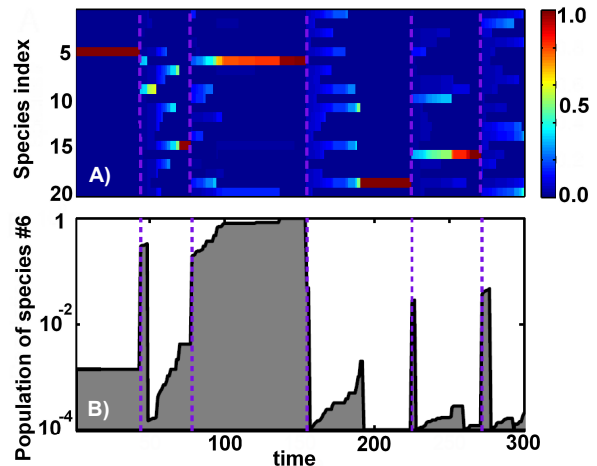


FIG. 1. (A) An example of the population dynamics in our model with $N = 20$ and $\gamma = 10^{-4}$. The color denotes sizes of local populations of species (see the colorbar on the right) with dominating species visible as red horizontal bands. Note five diversity waves ending at purple dashed lines. Transitions between these waves are triggered by the extinctions of the dominating species # 5, 15, 6, 19, 16 correspondingly. (B) The time-course of the species # 6 with the logarithmic y-axis. Note the pattern of intermittent exponential growth periods fuelled by local extinctions.

capacity of the environment is nearly exhausted by just one dominant species with $P_{max} \simeq 1$. When such dominant species goes extinct a large fraction of the resources suddenly becomes available and consequently all other populations increase by a large ratio $1/(1 - P_{max})$. This marks the end of one and the start of another diversity wave that initially is dominated by a large number of species with similar population sizes. In the course of this new wave these species are eliminated one-by-one by random extinctions until only one dominant species is left standing. Its collapse ends the current and starts the new wave. In Fig. 1A one can clearly distinguish about 5 such waves terminated by the extinctions of species #5, 15, 6, 19, and 16 correspondingly.

Fig. 1B shows the time-course of just one local population of the species #6 on a logarithmic scale. Between timesteps 100 and 150 the population of this species nearly exhausts the carrying capacity of the environment. Its local extinction at the timestep 154 ended the third di-

versity wave and started the fourth one. Note somewhat erratic yet distinctly exponential growth of this species happening on the slow timescale set by the frequency of extinctions. This growth should not be confused with exponential re-population of recently collapsed environments that happens much faster (a small fraction of one timestep).

Fig. 2 follows the population diversity (grey shaded area) defined as $D(t) = 1/\sum_{i=1}^N P_i(t)^2$ as a function of time in a system of size $N = 1000$. In general D can vary between ~ 1 when one abundant species dominates the environment and N when all species are equally abundant. The diversity is inversely proportional to the largest population $P_{max}(t) = \max_i P_i(t)$. The diversity waves (purple dashed arrows in Fig. 2) are initiated when a dominating species collapses. As a consequence, at the start of each wave the diversity abruptly increases from ~ 1 to a substantial fraction of the maximal possible diversity N . After this initial burst triggered by the global redistribution of biomass, the diversity exponentially declines as $\exp(-t/N)$ (the dot-dashed line in Fig.2), driven by ongoing extinctions of individual populations. The typical duration, t_{wave} of a diversity wave is equal to the time required for all of the species present at the start of the wave to go extinct one-by-one. Thus it is determined by $N \cdot \exp(-t_{wave}/N) \sim 1$ or

$$t_{wave} \sim N \cdot \log_e N \quad . \quad (2)$$

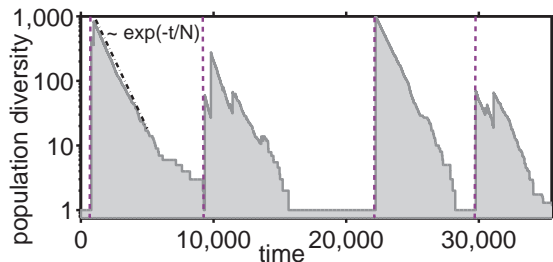


FIG. 2. The grey shaded area shows the the time course of the population diversity $D = 1/\sum_i P_i^2$ in our model with $N = 1000$ and $\gamma = 10^{-12}$. Purple dashed lines mark the beginnings of diversity waves when a collapse of the dominant species with $P_{max} \simeq 1$ leads to an abrupt increase in population diversity from ~ 1 to $\sim N$. The diversity subsequently decreases $\propto \exp(-t/N)$ (dash-dotted line)

Fig. 3 shows the compound distribution of population sizes for $\gamma = 10^{-9}$ and $N = 1000$ (the grey shaded area). This logarithmically-binned distribution defined by $\pi(P) = d\text{Prob}(P_i(t) > P)/d\log_{10} P$ were collected over 20 million individual collapses (time-steps in our model). Thus, a compound distribution is rather different from a typical “snapshot” of the system at a particular moment in time characterized by between 1 and N of highly abundant species in the current diversity wave. The compound distribution is bimodal with clearly separable peaks corresponding to two population subgroups.

The upper peak consists of the species that have not yet been eliminated in the current wave.

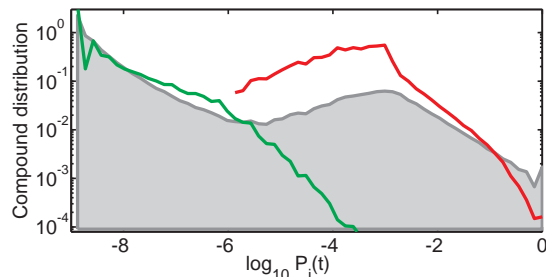


FIG. 3. The compound distributions of population sizes across time and space in our model with $\gamma = 10^{-9}$ and $N = 1000$ (grey shaded area). The green and red lines show the population distributions collected at the very end of each wave and at the very beginning of the next wave correspondingly as described in the text. Note that they roughly correspond to two peaks of the compound distribution.

To better understand the dynamics of the system in Fig. 3 we also show the distribution of populations sizes at the very end of each diversity wave (green line) and at the beginning of the next wave (red line). That is to say, for the green curve we take a snapshot of all populations immediately after the dominant species with $P_{max} > 1 - 1/N$ was eliminated, but before the available biomass was redistributed among all species. At those special moments, happening only once every t_{wave} time steps, most population sizes are between γ and $\gamma \cdot N$ while a small fraction reaches all the way up to $\sim 1/N$. During the rapid growth phase immediately after our snapshot was taken, all populations grow by the same factor $1/(1 - P_{max}) \simeq N$ thereby moving all of them to the upper peak of the compound distribution thereby starting the new wave. The red curve corresponds to the snapshot of all populations immediately after this rescaling took place. It shows that at the very beginning of the new wave local populations are broadly distributed between $\sim N \cdot \gamma$ and 1 with a peak around $1/N$.

Fig. 4A shows compound distributions of population sizes for $\gamma = 10^{-10}$ and different values of N ranging between 100 and 10,000 while Fig. 4B shows compound distributions with $N = 1000$ and for a wide range of γ . One can see that for $\gamma < 0.01/N$, the tail of the distribution for most abundant populations between $1/N$ and 1 is well fitted by a power law $\pi(P) \propto 1/P^{\tau-1} \simeq 1/P^{0.7}$ (dashed line in Fig. 4B) corresponding to the power law distribution of population sizes on the linear scale $d\text{Prob}(P_i(t) > P)/dP \sim 1/P^\tau \simeq 1/P^{1.7}$. Overall Figs. 4A,B demonstrate that the exponent τ for different values of γ and N is remarkably universal. Indeed, for a range of parameters where the upper and the lower peaks of $\pi(P)$ are clearly separated, τ varies only between 1.6 and 1.8 (larger values of τ correspond to larger systems and larger values of γ).

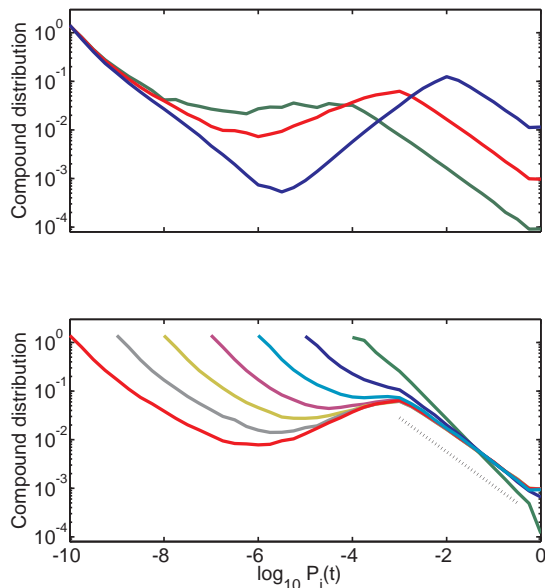


FIG. 4. Compound distributions of population sizes across time and space in our model with A) $\gamma = 10^{-10}$ and $N = 100$ (blue), $N = 1000$ (red), and $N = 10,000$ (green). B) $N = 1000$ and varying γ ranging between 10^{-4} (green) to 10^{-10} (red) in ten-fold decrements. Note the emergence of a nearly universal scale-free tail of the distribution fitted with $\tau \simeq 1.7$ (dashed line).

Discussion

In this paper we explore the population dynamics in saturated environments driven exclusively by near-complete collapses of sub-populations of competing species. This type of dynamics strongly contrasts the gradual changes implied in for example the “community drift” neutral models [5] in ecology, or for the most part incremental random walks of stock values of individual companies. Conversely, collapse driven dynamics represents a sudden and usually large change of system composition. In microbial ecology such collapse may be caused e.g. by invading bacteriophages, whereas in the economy even big companies routinely go bankrupt e.g. through excessive debt amplifying the effects of external perturbations.

First, let us consider sudden collapses or local extinctions in biological systems. Here sudden population-scale changes can occur e.g. due to introduced diseases or the disappearance of a key-stone species [11, 12] that changes the composition of the entire food-web. On the microbial scale, sudden invasion of a new bacteriophage may lead to multiple orders of magnitude reduction in the population of susceptible bacteria [8, 13], potentially leading to their complete local extinction [9]. Phage-driven collapses do not spare bacteria with large populations and may even be biased towards such as they represent easy and attractive targets for phages [14]. The compositions of abun-

dant marine bacterial strains are shown to vary widely between different locations along the Gulf Stream in the mid-Atlantic region [15, 16]. This hints at fast reshuffling of dominant populations in those environments driven by phages.

On a very different, geological timescale collapse-driven dynamics in our model resembles that of species extinctions and subsequent radiations in the paleontological record [17, 18]. One well documented example is the recolonization by mammals of a number of ecological niches vacated by dinosaurs after the end-Cretaceous mass extinction. Interestingly, the extinction rate of taxonomic orders appears to be independent of the size of the order quantified by the number of genera it contains [10] which is assumed in our basic model of collapse-driven dynamics.

The second area of applications of our model is to describe company dynamics in economics. The size or the market share of a publicly traded company reflected in its stock price is well approximated by a random walk with (usually) small incremental steps [19]. However, as in the case of ecosystems, this smooth and gradual drift does not account for dramatic rapid changes such as bankruptcies or market crashes. In case of companies the main driver of sudden changes is their debt [20]. When the intrinsic value of a company is much smaller than its debt, even small changes in its economical environment can make it insolvent not sparing even the biggest companies from bankruptcies (think of Enron and Lehman Brothers). Empirically, the year-to-year volatility of company’s market share varies with its size S , $\Delta S/S \propto S^{-0.2}$ [21].

Abundance distributions in our original model (see Fig. 3) and most of its variants are characterized by a power-law tail with an exponent τ between 1.5 and 2. This is in approximate agreement with the empirical data on abundance distributions of bacteria in soil samples [22], marine viruses (phages) [23], characterized by power-law tails with exponents close to 2.

In the economics literature, the distributions of company sizes [24] as well as those of individual wealth [25] are known to have similar scale-free tails. Recent data for companies [24] and personal wealth [25] suggest $1/P^{1.8}$ tail of the former distribution and $1/P^{2.3}$ tails of the latter one. Traditionally, scale-free tails in these distributions were explained by either stochastic multiplicative processes pushed against the lower wall (the minimal population or company size, or welfare support for low income individuals) [26–28], by variants of rich-get-richer dynamics [29], or in terms of Self-Organized Criticality [30, 31]. The emphasis of the latter type of models on large system-wide events (avalanches [30, 31] or collapses [32]) and on separation of timescales is similar in spirit to collapse-driven dynamics used in this study.

Needless to say, the model described in this paper was simplified in order to compare and contrast the collapse-driven dynamics to other mathematical descriptions of competition in saturated environments. In supplementary materials we describe several variants of our basic

model that in addition to population collapses include the following elements:

1. Neutral “random drift” changes of population sizes during time intervals between collapses described in Ref. [5]. In this model in addition to collapses a population of size P_i drifts up and down $\Delta P_i \propto \pm\sqrt{P_i(1-P_i)}$. The resulting diversity waves and compound distributions can be found in the supplementary Fig. S1.
2. Another variant of the neutral model is when population sizes between collapses undergo slow multiplicative adjustments $\Delta P_i \propto \pm\Omega_i P_i$ restricted by the overall carrying capacity of the environment. Details and the resulting compound distribution can be found in the supplementary Fig. S2.
3. We also consider another neutral variant of our basic model in which spatially separated sub-populations of the same species are competing with each other for the same nutrient. Sub-populations are connected by the diffusion, that is much slower than the diffusion of shared nutrient. In this model a collapsed sub-population is replenished by a small number γ of individuals diffusing from other environments, see the supplementary Fig. S3
4. In the next variant we allow the collapse probability c to systematically decrease with the population size P as $c(P) \sim P^{-0.2}$ as suggested by the empirical studies of company dynamics [21]. As seen in the supplementary Fig. S4 the diversity dynamics and the scale-free tail of the population distribution are both remarkably robust with respect to introduction of size-dependent collapse rate.
5. A model in which each of the species has its own fitness quantified by its growth rate Ω_i during rapid re-population phase and its collapse probability c_i . The supplementary Fig S5 show that the overall shape of the compound distribution is similar to that in our basic model, whereas its lower panel illustrate the interplay between population size and the two variables that define the species’ fitness.
6. We finally consider another fitness model in which collapsing species do not necessarily go into extinction. Instead, each species is assigned its own “survivor ratio” γ_i defined by the population drop following a collapse: $P_i \rightarrow \gamma_i P_i$. As in the previous variant each of the species is also characterized by its own growth rate Ω_i . The supplementary Fig S6 shows that for intermediate populations the compound distribution is described by a power law scaling. Compared to the basic model it has a broader scaling regime and larger likelihood to have most of the “biomass” collected in one species.

Captions to supplementary figures S1-S6 provide more detailed description of model dynamics in each of these

cases. Overall, the simulations of the six variants of our basic model described above preserve the general patterns of collapse-driven dynamics such as diversity wave dynamics, and a broad compound distribution of population sizes with scale-free tail for the most abundant species.

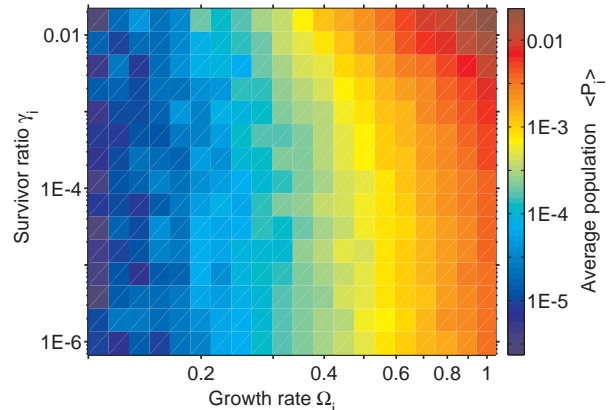


FIG. 5. *Time-averaged population of a species (see colorbar on the right) plotted as a function of its re-population growth rate Ω_i (x-axis) and population drop after collapses γ_i (y-axis), in a variant of our model with fitness differences between species. Note that the population increase with both Ω_i and γ_i . Populations and fitness parameters of $N = 1000$ species were taken from 50 million snapshots of the model.*

A traditional definition of the fitness of a species in terms of its long-term exponential growth rate is clearly inappropriate for our model. Indeed, the long-term growth rate of each of our species is exactly zero. A better way to quantify species’ success in a steady state system like ours is in terms of their average population size $\langle P_i(t) \rangle$. In the last two variants of our basic model we add fitness-related parameters to each of the species: its short-term exponential growth rate Ω_i (model 5 and 6), its propensity to large population collapses quantified by their frequency c_i (model 5), and the severity of collapses quantified by surviving fraction γ_i of the population (model 6). Fig. 5 shows the average population size $\langle P_i(t) \rangle_t$ as function of Ω_i and γ_i in the model 6. As one can naively expect species with larger short-term growth rates and larger surviving ratios also tend to have substantially larger populations (the red area in the upper right corner of Fig. 5).

While in our models the probability c_i and severity $1/\gamma_i$ of collapses are assumed to be independent of growth rate Ω_i in reality they are often oppositely correlated. Indeed, in biology much as in economics/finance fast growth usually comes at the cost of fragility and exposure to downturns forcing species to optimize trade-offs.

Some environmental conditions favor the fast growth even at the cost of a higher risk of collapse, whereas other

could call for sacrificing growth to minimize probability or severity of collapses. Species in frequently collapsing environments considered in our study are known to employ bet-hedging strategies [2, 33–35] to optimize their long-term growth rate. This is obtained by splitting their populations into “growth-loving” and “risk-averse” phenotypes [34–36]. One example of this type of bet-hedging is provided by persister sub-populations of some

bacterial species consisting of $\gamma \sim 10^{-4}$ of the overall population [37, 38] increasing to as much as $\gamma = 10^{-2}$ in saturated conditions (S. Semsey, private communications). A bet-hedging strategy with persister sub-population 10^{-2} somewhat reduces the overall growth rate (only by 1%) while dramatically reducing the severity of collapses caused by antibiotics. From Fig. 5 one infers that this is indeed a good trade-off.

-
- [1] Fisher RA (1930) *The Genetical Theory of Natural selection*. Clarendon, Oxford
- [2] Kelly JL (1956) A new interpretation of information rate. *Bell System Technical Journal* 35:917-926
- [3] Malthus TR (1798) *An Essay on the Principle of Population*. J. Johnson, in St. Paul’s Church-yard, London
- [4] Verhulst PF (1838) Notice sur la loi la population poursuit dans son accroissement. *Correspondance Mathématique et Physique*, 10: 113-121
- [5] Hubbell SP (2001) *The unified neutral theory of biodiversity and biogeography* (MPB-32), Princeton University Press
- [6] Woodcock S, Gast VC (2007) Neutral assembly of bacterial communities. *FEMS Microbiol Ecol* 62: 171–180
- [7] Sloan WT, Lunn M, Woodcock S (2006) Quantifying the roles of immigration and chance in shaping prokaryote community structure. *Environmental Microbiology*, 8: 732–740
- [8] Middelboe M, Hagström A, Blackburn N, Sinn B, Fischer U, et al. (2001) Effects of Bacteriophages on the Population Dynamics of Four Strains of Pelagic Marine Bacteria. *Microb Ecol* 42: 395–406; doi:10.1007/s00248-001-0012-1
- [9] Haerter JO, Mitarai N, Sneppen K (2014) Phage and bacteria support mutual diversity in a narrowing staircase of coexistence. *The ISME journal*. *The ISME Journal* 8: 2317-2326
- [10] Bornholdt S, Sneppen K, and Westphal H (2009) Longevity of orders is related to the longevity of their constituent genera rather than genus richness. *Theory in Biosciences* 128: 75-83
- [11] Paine RT (1969) A note on trophic complexity and community stability. *American naturalist* 103:91-93
- [12] Cohn JP (1998) Understanding Sea Otters. *BioScience* 48: 151–155
- [13] Levin BR, Stewart FM, and Chao L (1977) Resource-Limited Growth, Competition, and Predation: A Model and Experimental Studies with Bacteria and Bacteriophage., *The American Naturalist* 111: 3-24
- [14] Thingstad TF and Lignell R (1997) Theoretical models for the control of bacterial growth rate, abundance, diversity and carbon demand. *Aquatic Microbial Ecology* 13:19-27
- [15] Moebus K, Nattkemper H (1981) Bacteriophage sensitivity patterns among bacteria isolated from marine waters. *Helgoländer Meeresuntersuchungen* 34: 375-385
- [16] Flores CO, Valverde S, Weitz JS (2013) Multi-scale structure and geographic drivers of cross-infection within marine bacteria and phages. *The ISME journal* 7: 520–532
- [17] Raup DM. (1992) Extinction: bad genes or bad luck? WW Norton and Company.
- [18] L. Van Valen. A new evolutionary law. *Evolutionary Theory*, 1:1, (1973).
- [19] Bachelier L. (1900) *Théorie de la spéculation*. Gauthier-Villars, 70 pp.
- [20] Fisher I (1933) The debt-deflation theory of great depressions. *Econometrica* 1:337–357.
- [21] Nunes Amaral LA, Buldyrev SV, Havlin S, Leschhorn H, Maass P, Salinger MA, et al. (1997) Scaling Behavior in Economics: I. Empirical Results for Company Growth. *Journal de Physique I*. 7: 621–633.
- [22] Gans J, Wolinsky M and Dunbar J (2005) Computational Improvements Reveal Great Bacterial Diversity and High Metal Toxicity in Soil. *Science* 309: 1387–1390
- [23] Breitbart M et al. (2002) Genomic analysis of uncultured marine viral communities. *PNAS* 99: 14250–14255
- [24] Filiassi M, Livan G, Marsili M, Peressi M, Vesselli E and Zarinelli E (2014) On the concentration of large deviations for fat tailed distributions, with application to financial data. *Journal of Statistical Mechanics: Theory and Experiment* P09030.
- [25] Klass OS, Biham O, Levy M, Malcai O and Solomon S (2006) The Forbes 400 and the Pareto wealth distribution. *Economics Letters* 90: 290-295.
- [26] Levy M and Solomon S (1996) Power laws are logarithmic Boltzmann laws. *International Journal of Modern Physics C* 7:595-601
- [27] Levy M and Solomon S (1997) New evidence for the power-law distribution of wealth. *Physica A* 242:90-94
- [28] Sornette D and Cont R (1997) Convergent multiplicative processes repelled from zero: power laws and truncated power laws.” *Journal de Physique I* 7:431-444
- [29] Simon HA (1955) On a class of skew distribution functions. *Biometrika* 42:425-440
- [30] Bak P, Tang C, Wiesenfeld K (1987) Self-organized criticality: An explanation of the $1/f$ noise. *Physical Review letters*, 59(4): 381-384.
- [31] Bak P and Sneppen K (1993) Punctuated Equilibrium and Criticality in a simple model of Evolution. *Phys. Rev. Lett.* 71: 4083–4086.
- [32] Newman MEJ and Sneppen K (1996) Avalanches, scaling, and coherent noise. *Physical Review E* 54: 6226-6231
- [33] Maslov S, Zhang Y-C (1998) Optimal investment strategy for risky assets. *International Journal of Theoretical and Applied Finance* 1: 377–387
- [34] Bergstrom CT and Lanhman M (2004) Shannon Information and Biological Fitness. *Proceedings of the Information Theory Workshop, IEEE* 0-7803-8720-1: 50-54; available at doi:10.1109/ITW.2004.1405273
- [35] Maslov S and Sneppen K (2015) Well-temperate phage: optimal bet-hedging against local environmental collapses. *Scientific Reports* (submitted);

- <http://arxiv.org/abs/1308.1646>
- [36] Kussell E, Kishony R, Balaban N-Q and Leibler S (2005) Bacterial persistence a model of survival in changing environments. *Genetics* 169: 1807-1814
- [37] Balaban NQ, Merrin J, Chait R, Kowalik L and Leibler S (2004) Bacterial persistence as a phenotypic switch. *Science* 305: 1622-1625
- [38] Maisonneuve E, Castro-Camargo M and Gerdes K (2013) (p)ppGpp controls bacterial persistence by stochastic induction of toxin-antitoxin activity. *Cell* 154:1140-1150.

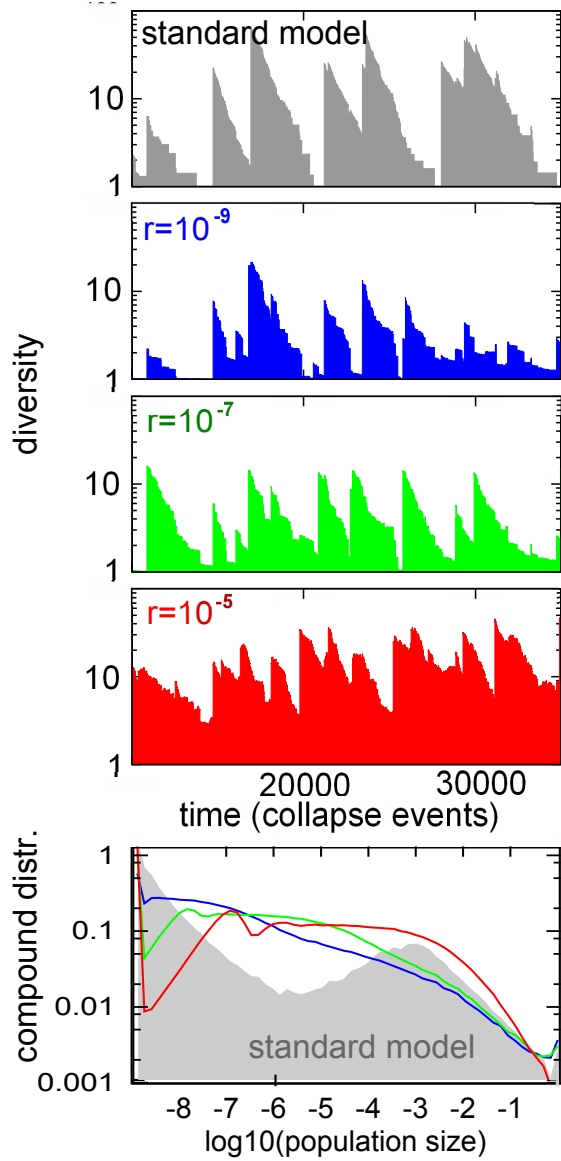


FIG. S1. The neutral “random drift” model. This variant extends our basic model with $N = 1000$ and collapse ratio $\gamma = 10^{-9}$ by adding neutral drift at rate r taking place between subsequent collapse events in our standard model. To simulate neutral drift at every time step the population of each species is changed according to $P_i \rightarrow P_i \pm \sqrt{r \cdot P_i(1 - P_i)}$, while preserving the overall $\sum P_i = 1$ (and constraining $P_i \geq \gamma$). This is followed by a collapse event where one of the species is randomly selected and its population is reset to $P_i \rightarrow \gamma$ and subsequently all species are rescaled to the carrying capacity $\sum P_i = 1$. The lower panel shows the compound distributions in our system simulated for 10^6 collapse events. The grey shaded area refers to our basic, unmodified model, i.e. to the $r = 0$ case, while three color lines correspond to $r = 10^{-9}$ (blue), $r = 10^{-7}$ (green), and $r = 10^{-5}$ (red). The upper four panels illustrate typical time courses of the diversity $D(t) = 1/\sum P_i(t)^2$ in our basic model and three values of the r color-coded as in the lower panel. Note that for simplicity of simulation we simulations in this variant of the model we ignore the exponential distribution of time interval τ_r between subsequent collapse events and use $\tau_r = 1$ instead.

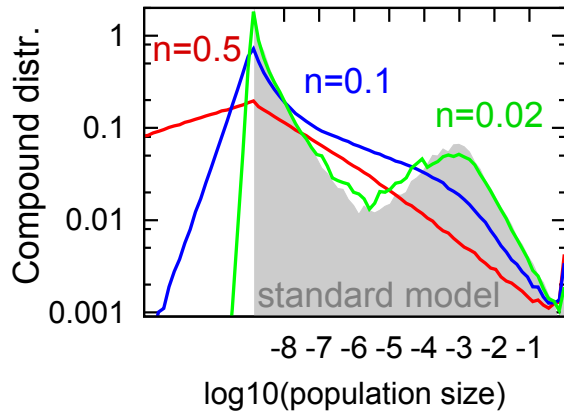


FIG. S2. Model with random exponential redistribution of populations taking place between collapse events. The time interval τ_r elapsed between two subsequent collapse events is randomly chosen at each time step from an exponential distribution with mean value equal to 1. Each species population is subject to a random growth, $P_i \rightarrow P_i \cdot e^{n \cdot \tau_r \cdot \text{rand}_i(t)}$ and subsequently rescaled to the carrying capacity of the environment: $\sum P_i = 1$. Here n quantifies the overall rate of the redistribution, while $\text{rand}_i(t)$ - a random number between 0 and 1 - represents species- and time step-specific component of growth rates. Its value is reselected for every species after every collapse events. Such stochasticity in growth rates captures all possible contingencies and species-specific fluctuations in growth conditions. As in our basic model, at every time step one population i randomly collapses and reset to $P_i \rightarrow \gamma = 10^{-9}$ and all populations are rescaled to fulfill $\sum P_i = 1$. The figure examines a $N = 1000$ system simulated for 10^6 collapse events. The grey shaded area refer to the standard model, corresponding to the $n = 0$ case.

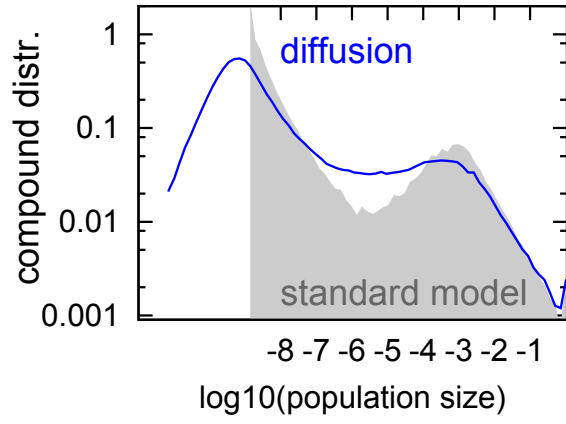


FIG. S3. Model with diffusion between multiple environments. In this version of the model we simulate populations of a **single** species distributed between $N = 1000$ different environments connected by diffusion. At each time step a fraction $\gamma = 10^{-9}$ of the total population is assumed to diffuse freely between these environments. One population i is selected for collapse and reset to $P_i \rightarrow 0$ after which all populations are seeded equally by diffusion: $P_i \rightarrow P_i + \gamma/N$. All populations are then grow at identical rates until they reach a global carrying capacity: $\sum P_i = 1$. Note, that here we implicitly assume that populations in all of these environments share the same carrying capacity. This is the case when diffusion rate of the rate-limiting nutrient is much faster then that of populations themselves. The histograms shown here were obtained by simulating for 10^6 subsequent collapse events. The grey shaded area refer to the standard model, i.e. where the just-collapsed population (and no other populations) is assigned a seed population of size γ .

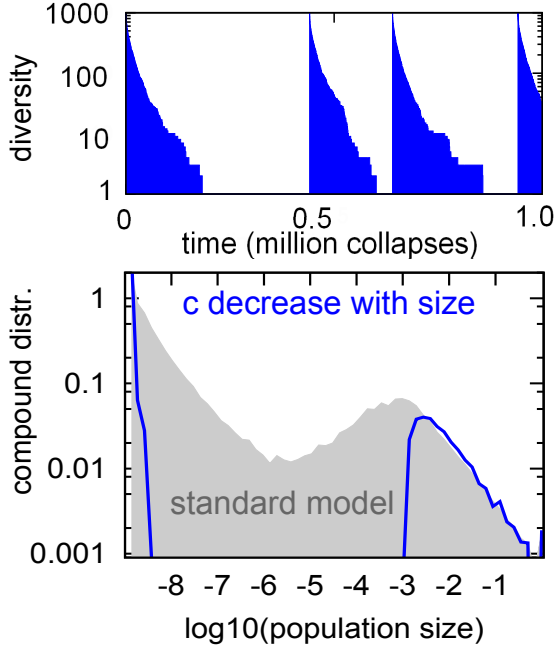


FIG. S4. Model with a collapse probability declining with population size in a power-law fashion. At each time step we select a random population to collapse with probability $\propto P_i^{-0.2}$ decreasing with its size. In economics this corresponds to an intuitive notion that larger companies are less likely to go bankrupt than smaller ones. Empirically, this trend is described by a power law with exponent -0.2 (Nunes Amaral LA, Buldyrev SV, Havlin S, Leschhorn H, Maass P, Salinger MA, et al. (1997) *Scaling Behavior in Economics: I. Empirical Results for Company Growth*. *Journal de Physique I*. 7: 621–633.) For bacterial populations the direction of the trend (if any) of collapse probability with population size is currently unknown. In fact one can plausibly make a case for increasing of the probability of collapse with population size due to larger populations making easier to find and overall and more attractive targets for phages. In our model the collapsing population is reset to $P_i \rightarrow \gamma = 10^{-9}$ and all populations are subsequently grown with equal exponential rates to complete saturation: $\sum P_i = 1$. The figure examines an $N = 1000$ system simulated for 10^6 collapse events. The upper panel illustrates the recurrent diversity waves, whereas the lower panel show the compound distribution, with the grey shaded area referring to our standard model. Notice the emergence of a much more narrow distributions around γ than in the standard model. This makes sense as in the course of the wave small populations tend to collapse first. Their collapses don't drive other populations up by much and thus they all end up clustering close to each other at the very bottom of the next wave distribution around γ . When the dominant population finally collapses all small populations are rescaled up to form a narrow distribution around $1/N$. This starts a new diversity wave with diversity $D(t) \sim N$ which is subsequently reduced with time as $D(t) \propto \exp(-t/N)$ if we ignore the relatively small $N^{0.2}$ -fold change in collapse frequency when changing population sizes from $1/N$ to N . In this approximation, each surviving population grows as $P(t) \propto \exp(t/N)$. The time-averaged distribution of populations thereby approaches the scaling $\text{Prob}(P_i(t) > P) \sim \frac{1}{P} \Rightarrow \frac{d\text{Prob}(P_i(t) > P)}{dP} \sim \frac{1}{P^2}$. In reality the scaling exponent of the tail is around 1.8. It is the same as in our standard model but for a different reason. Indeed, taking into account that lifetime of a population before collapse scales as $1/P^{-0.2} = P^{0.2}$ one gets $\text{Prob}(P_i(t) = P) \sim \frac{P^{0.2}}{P^2} = \frac{1}{P^{1.8}}$.

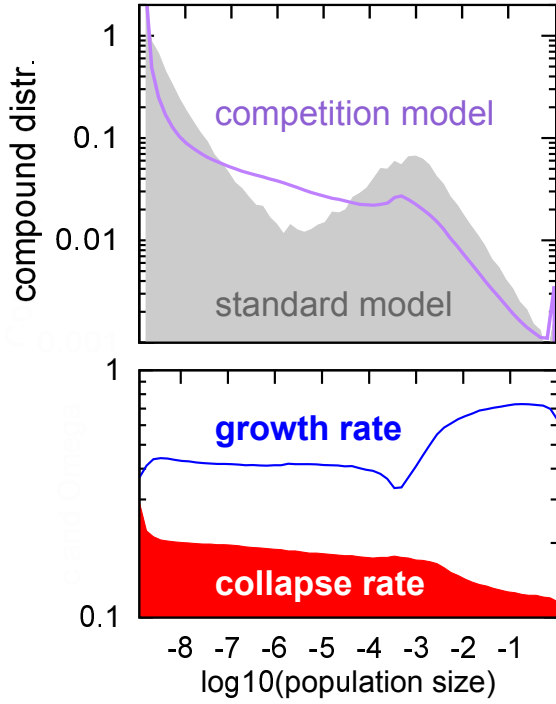


FIG. S5. Model with heterogeneous, species-specific growth rates and extinction probabilities. Each species is assigned a growth rate Ω_i used when it repopulates the freed-up carrying capacity of the environment. It also has its own collapse probability c_i . Both Ω_i and $\log_{10}c_i$ are logarithmically distributed in the interval between 0.1 and 1. At each time step we randomly select one of the N populations, with probability $\propto c_k$, and collapse its population as $P_k \rightarrow \gamma = 10^{-9}$. Subsequently all of the populations $i = 1, 2, \dots, N$ are rescaled up $P_i \rightarrow P_i + (P_k - \gamma) \cdot \frac{\Omega_i P_i}{\sum_j \Omega_j P_j}$ to fill up the carrying capacity of the environment: $\sum P_i = 1$. The collapsed population is assigned a new random growth rate Ω_i and a new collapse probability c_i . The purple curve in the upper panel shows the compound population distribution whereas the grey shaded area is that for the standard model where all growth and collapse rates are equal. The lower panel shows the average collapse probability and growth rate binned by the size of the population. Populations larger than $1/N = 0.001$ tend to have smaller than average c_i and larger than average growth rates Ω_i .

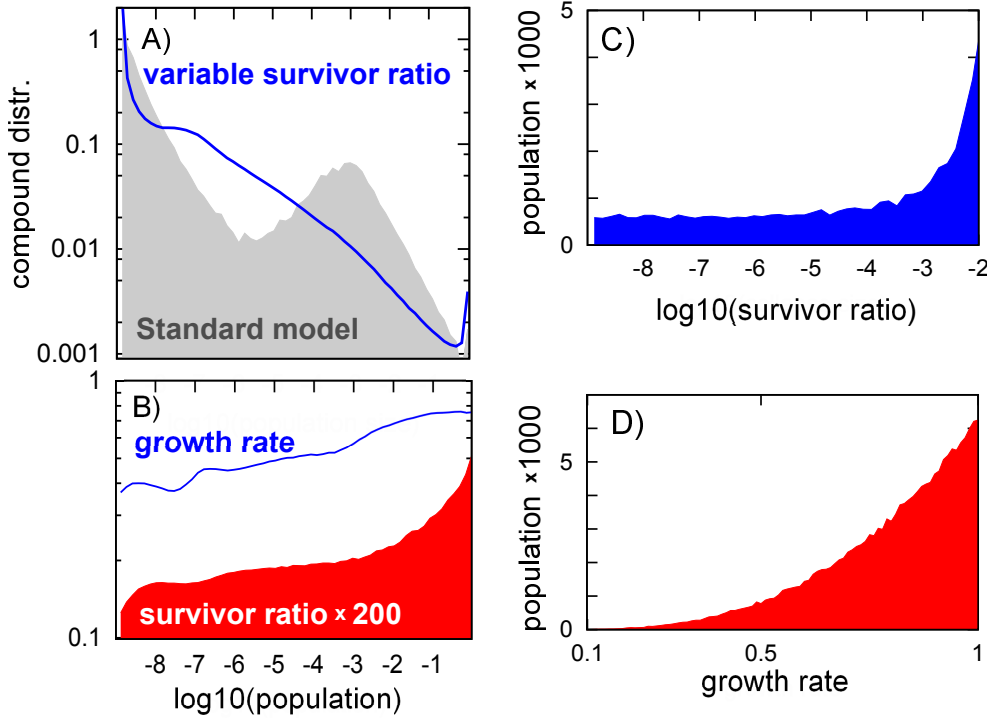


FIG. S6. Model with heterogeneous, species-specific growth rates and survival ratios (collapse sizes). Each species is assigned a growth rate $\Omega_i \in [0.1, 1]$ and collapse size $\gamma_i \in [10^{-9}, 10^{-2}]$, both logarithmically distributed. At each time step we select one of the N populations, and reset its population $P_k \rightarrow \gamma_k \cdot P_k$. Note that unlike in previous versions we scale down the population proportional to its size and not proportional to the carrying capacity of the environment. This is because our interpretation is different in this case. In this version of the model collapse represents a sudden and dramatic reduction of its population. This should be contrasted to other versions where each collapse represented a complete extinction of the species followed by appearance of a new species with a small population γ . In this version of the model extinction happens only if $\gamma_k P_k < 10^{-9}$. In this case old species goes extinct and the new species appears with the initial population $P_k = \gamma_{new} = 10^{-9}$. The new species is assigned new random values of Ω_k and γ_k . Subsequently all populations $i = 1, 2, \dots, N$ are rescaled $P_i \rightarrow P_i + (P_k - \gamma) \cdot \frac{\Omega_i P_i}{\sum_j \Omega_j P_j}$ to fill up the carrying capacity of the environment: $\sum P_i = 1$. A) The blue curve shows the population distribution, whereas the grey area refers to our standard model from the main text. B) The average growth rate $\langle \Omega_i \rangle$ and the average survivor ratio $\langle \gamma_i \rangle$ (multiplied by 200 to have the same range in the plot) binned by the population size. C) The average population size binned by the survivor ratio γ_i of the species. D) The average population size binned by the growth rate Ω_i of the species.